Nondestructive Testing of Overhead Transmission Lines

Stephanie L. Branham, Mike S. Wilson, Stefan Hurlebaus
Zachry Department of Civil Engineering
Texas A&M University
College Station, TX, 77843-3136
email: shurlebaus@civil.tamu.edu

Brad M. Beadle, Lothar Gaul
Institute of Applied and Experimental Mechanics
University of Stuttgart
Pfaffenwaldring 9, 70550 Stuttgart
email: gaul@iam.uni-stuttgart.de

ABSTRACT

Overhead power lines are periodically inspected using both on-ground and helicopter-aided visual inspection. Factors including sun glare, cloud cover, close proximity to power lines, and rapidly changing visual circumstances make airborne inspection of power lines a particularly hazardous task. In this study, the feasibility of continuous, on-line monitoring of power lines using ultrasonic waves is considered. A sending/receiving transducer located on the power line generates an ultrasonic wave in the cable. A defect in the cable will cause a portion of the incident ultrasonic wave to be reflected back to the transducer. Data acquired by the transducer can be relayed to a central communication node via a wireless transmitter. The methodology developed in this study can also be applied to other cable monitoring applications, such as bridge cable monitoring, which would otherwise put human inspectors at risk.

Keywords: transmission line, Pochhammer bar, longitudinal waves, piezoelectric transducers

1. INTRODUCTION

Multi-wire cables find wide use in a number of engineering applications. For example, they are used for pre-stressing and post-tensioning in concrete structures; they serve as the load-carrying structures on cable-stayed and suspension bridges; they are found on elevators; and, they form the transmission lines which deliver power to our homes and businesses. Monitoring the integrity of these cables becomes increasingly important as the cable ages. This study focuses in particular on the structural health monitoring of overhead transmission lines.

Common failures associated with overhead power line installations include broken insulators, broken lightening rods, loose earth conductors, loose spacers (spacers are used to separate individual lines), and uncoiled or broken cable wires caused by wind-induced vibrations (Siegert and Brevet, 2005). Power line installations are periodically inspected using both on-ground and helicopter-aided visual inspections. Factors including sun glare, cloud cover, close proximity to power lines, and rapidly changing visual circumstances make airborne inspection of power lines a particularly hazardous task. Such factors have led to a number of fatal helicopter crashes in recent years. A summary of the helicopter accidents due to aerial observation is depicted in Table. 1 (U.S. Helicopter Summary Statistics, 1996-2004).

The risk associated with aerial inspection of power line installations could be substantially reduced through partial automation of the inspection process. The power lines themselves could be automatically monitored. Aerial and ground inspections could then focus on identifying problems associated only with the mast structures. Introduction of such an inspection approach not only reduces risks to human pilots, but it also speeds up the inspection process. The methodology developed in this study can also be applied to other cable monitoring applications, which would otherwise put human inspectors at risk.

Table 1: Summary of helicopter accidents due to aerial observation.

	1996	1997	1998	1999	2000	2001	2002	2003	2004
Total Accidents	176	163	191	197	206	182	205	214	180
Fatal Accidents	32	27	34	31	35	29	26	37	33
Fatal Injuries	54	43	66	57	63	51	41	67	68
FAR 91 Aerial Observation	10	6	6	13	7	5	8	8	9

The basic idea for defect detection in a transmission line is illustrated in Fig. 1. As shown, a transducer is used to both generate and detect ultrasonic bursts in the power line. Initially, longitudinal waves will be used for diagnostic purposes. When the ultrasonic burst interacts with a defect, such as a broken wire, a portion of the incident wave will be reflected. The reflected wave is then sensed by the receiving transducer. If the amplitude of the reflected wave is above a certain threshold value, then positive identification of a defect can be assumed. A wireless transmitter located at the transducer could be used to relay data to a central communication node or to a defect indicator located on the mast.

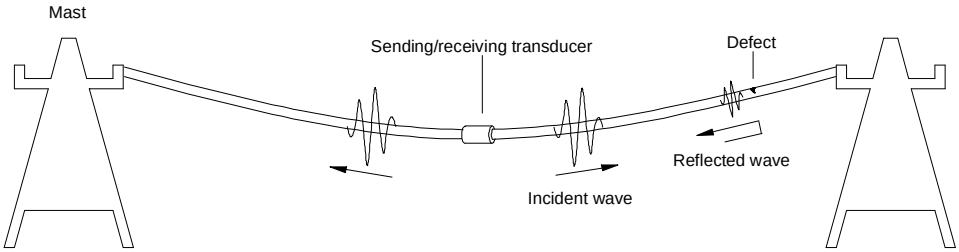

Fig. 1: Interrogation of a transmission line using ultrasonic pulses

2. SURVEY OF RELEVENT WORK

Meitzler (1961) studied the propagation of elastic pulses in wires having a circular cross section. He attributed pulse distortion to the propagation of several modes. His experimental and theoretical results suggest that coupling between the various modes of propagation were responsible for the observed pulse distortion. Rizzo and Lanza di Scalea (2002) generated and detected ultrasonic waves in single wires and seven-wire cables using magnetostrictive sensors. A formulation based on the Pochhammer-Chree theory is used to predict the change in the velocity of longitudinal waves as a function of applied stress (acoustoelastic effect). Results from acoustoelastic experiments are presented and compared to the theoretical predictions. Ways to enhance the sensitivity of the acoustoelastic measurements were investigated. The different behavior exhibited by the seven-wire cables when compared to single wires suggests the need for widening the theory to include acoustoelastic phenomenon in multi-wire cables. Additionally, the suitability of the guided wave method for the detection of defects in the critical anchorage zones is considered. Washer et al. (2002) also utilized the acoustoelastic effect for measuring the stress levels in post-tensioning rods and seven-wire cables. In a later study, Rizzo and Lanza di Scalea (2004) examined the wave propagation problem in seven-wire cables at the level of the individual wires. They used a broadband ultrasonic setup and a time-frequency analysis based on the wavelet transform for characterizing the dispersion and attenuation of longitudinal and flexural waves. They identified the vibration modes which propagate with minimal losses. Such modes are particularly useful for long-range inspection of the wires. Furthermore they found that since the dispersion curves are sensitive to the load level, the elastic waves could be used for

continuous load monitoring. In a recent paper, Rizzo and Lanza di Scalea (2005) employed a time-frequency analysis based on the discrete wavelet transform (DWT) for analyzing the ultrasonic signals. They found the de-noising property of the DWT to be particularly useful in their analyses.

3. THEORY

Ultrasonic waves are used for material characterization in many structural health monitoring and nondestructive evaluation applications. Guided ultrasonic waves are particularly effective for interrogating large structural components, since they propagate far distances when compared to body waves. Guided waves appear in a medium which constrains internal disturbances to move between the lateral bounding surfaces. In essence, standing waves are established in the lateral (short) direction whereas propagating waves are manifested in the normal (long) direction. For the case of a multi-wire cable, there exists no closed-form analytical solution which describes wave propagation. The following development therefore focuses on the simpler case of a single wire.

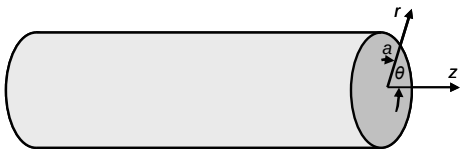

Fig. 2: Cylindrical rod with coordinates.

For the case of a solid, homogenous cylindrical rod with radius *a* (see Fig. 2), the substitution of the stress-free boundary conditions $\tau_{rr} = \tau_{r\theta} = \tau_{rz} = 0$ at the rod surface $r = a$ into the Lamé-Navier equations leads to the so-called Pochhammer frequency equation for the longitudinal modes (Graff, 1991),

$$\frac{2p}{a}\left(q^2+k^2\right)\mathrm{J}_1(pa)\mathrm{J}_1(qa)-\left(q^2-k^2\right)^2\mathrm{J}_0(pa)\mathrm{J}_1(qa)-4k^2pq\mathrm{J}_1(pa)\mathrm{J}_0(qa)=0\,. \qquad (1)$$

Here, J_0 and J_1 are Bessel functions of the first kind of orders 0 and 1 respectively; and, *p* and *q* are given by

$$p^2=\frac{\omega^2}{c_B{}^2}-k^2 \qquad q^2=\frac{\omega^2}{c_S{}^2}-k^2\,, \qquad (2)$$

where ω is the circular frequency, *k* is the circular wavenumber, c_B is the bulk wave speed in an unbounded medium, and c_s is the shear wave speed. The radial and axial displacements for the longitudinal modes are, respectively

$$u_r(r,z,t)=-\left[p\mathrm{J}_1(pr)+Cik\mathrm{J}_1(qr)\right]\mathrm{e}^{i(kz-\omega t)}$$
$$u_z(r,z,t)=\left[ik\mathrm{J}_0(pr)+Cq\mathrm{J}_0(qr)\right]\mathrm{e}^{i(kz-\omega t)} \qquad (3)$$
$$C=\frac{-2ikp}{q^2-k^2}\frac{\mathrm{J}_1(pa)}{\mathrm{J}_1(qa)}.$$

A similar analysis yields frequency equations and displacement mode shapes for torsional and flexural waves. This study however uses the fundamental longitudinal mode for defect identification. In the case of pulse-echo detection in which the ultrasonic source is also used as the receiver, as used in this study, the fundamental longitudinal mode is the fastest moving mode and can therefore be used for clear identification of defects. Fig. 3 depicts the group velocity-frequency characteristic for the first two longitudinal modes (L(0,1) and L(0,2)) and the first two flexural modes (F(1,1) and F(1,2)). The dispersion characteristic was calculated for the rods considered in this study (4.45 mm diameter, aluminum). At low frequencies, the group velocity of the fundamental longitudinal mode approaches the bar wave velocity $\sqrt{E/\rho}$; and at high frequencies, the group velocity approaches the Rayleigh wave velocity. The radial variation of axial stress as a function of frequency for the fundamental longitudinal mode is depicted in Fig. 4. The stress curves were computed using the displacement functions in Eqn. (3). The curves were normalized by setting the largest values of radial distance and stress to one. At high frequencies, the elastic energy becomes concentrated near the surface. This skin effect is found in plates and in the case of Rayleigh wave propagation in a half-space.

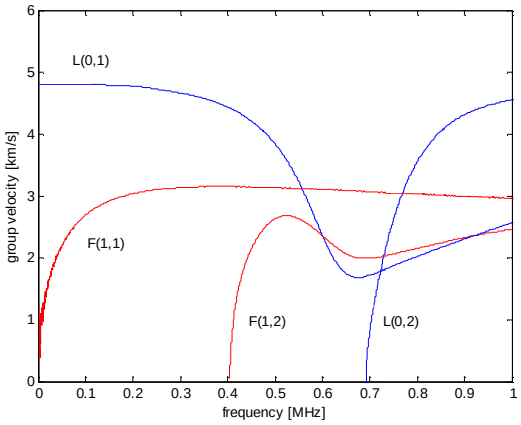

Fig. 3: Group velocity-frequency dispersion characteristic for a 4.45 mm diameter aluminum rod.

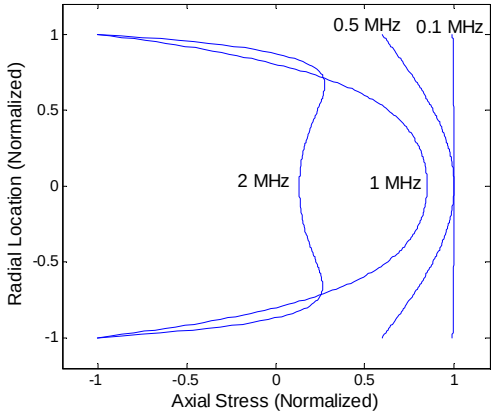

Fig. 4: Radial variation of axial stress for the 1st longitudinal rod mode.

The equation describing the longitudinal wave motion (Eqn. 3) does not account for attenuation due to material or geometrical effects. Introducing the complex wavenumber $k^* = k_1 + k_2 i$, the axial motion at a fixed radial distance can be expressed as

$$u_z(z,t) = A\mathrm{e}^{i\left(k^* z - \omega t\right)} = A\mathrm{e}^{-k_2 z}\mathrm{e}^{i(k_1 z - \omega t)}. \qquad (4)$$

It is clear from Eqn. (4) that the k_1 contribution is associated with propagation of the wave, and the k_2 contribution is associated with spatial attenuation of the wave. It follows immediately that

$$k_2 = \frac{1}{\Delta z}\ln\left|\frac{u_z(z,t)}{u_z(z+\Delta z,t)}\right|, \qquad (5)$$

where Δz is the separation distance between two measurement points.

4. EXPERIMENTAL CHARACTERIZATION OF THE 1ST LONGITUDINAL MODE

A cross-sectional view of the transmission line considered in this study is depicted in Figure 5. The transmission line is comprised of thirty-three steel and aluminum wires which are tightly wound together. There are seven load-bearing steel wires in the middle of the transmission line, which are surrounded by twenty-six current-carrying aluminum wires. The diameter of each steel wire is 3.5 mm, and the diameter of each aluminum wire is 4.45 mm. The diameter of the entire transmission line is 28.3 mm, and the length is 910 mm. In section 4.1, the experimental characterization of longitudinal waves in a single aluminum wire is presented. Specifically, the attenuation and dispersion behavior of the first longitudinal mode are determined. In section 4.2, the wave phenomenon in the transmission line as a whole is characterized. Cross-sectional measurements of the axial displacement are made in addition to attenuation and dispersion measurements.

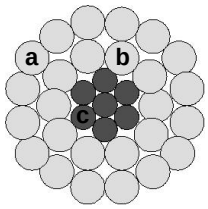

Fig. 5: Cross-sectional view of the transmission line.

4.1. Single Wire Measurements

The experimental setup for characterizing longitudinal mode propagation in a single wire is depicted in Fig. 6. A single sine burst from the function generator is amplified with the radio frequency (RF) amplifier, and this signal is used to drive a piezoelectric disc transducer. The transducer in turn generates an elastic wave in the aluminum wire (4.45 mm diameter, 820 mm length). The elastic wave propagates through the aluminum wire and is detected by a laser Doppler vibrometer (LDV). The LDV is a powerful measurement tool which allows non-contact, high fidelity, point-like measurements over a wide frequency range. As shown, the LDV is used to measure the axial particle velocity at the left end of the wire. The output from the LDV is captured by an oscilloscope and is then transferred to a PC for processing. Figure 7 depicts the measured axial particle velocity at the wire end for different frequencies. The existence of three discrete signal bursts (as seen in the 500 kHz trace) is evidence of the dispersive nature of the fundamental longitudinal mode. The frequencies of the bursts themselves coincide with the natural frequencies of the disc transducer.

The LDV is particularly well-suited to making attenuation measurements since it is non-contact and therefore does not influence wave propagation. The attenuation coefficient is estimated according to Eqn. (5), where the maximum amplitudes of the end reflections have been used in computations. Depicted in Fig. 8 is the LDV-measured axial velocity for a 100 kHz drive frequency. The attenuation coefficient of the first longitudinal mode at this excitation frequency is estimated to be $k_2 = 0.15\ m^{-1}$. Thus, the elastic wave will propagate approximately 30 m before the signal level falls below a measurable level, specifically when the signal-to-noise ratio (SNR) < 2. Obviously, this material damping estimate is somewhat high since the driving transducer partially absorbs the elastic energy.

4.2. Transmission Line Measurements

The experimental setup for measuring the longitudinal modes in a transmission line (28.3 mm diameter, 910 mm length) is depicted in Fig. 9. The transmission line setup is identical to the single wire setup, with the exception that a piezoelectric ring is used as the driving transducer. Fig. 10 depicts the measured axial particle velocity for a surface wire at different drive frequencies. There exists two discrete signals (as seen in the 500 kHz trace). The first signal corresponds to the fast-moving longitudinal mode, and the second signal corresponds to a slower-moving flexural mode. The dispersion of the second signal at low frequencies (as

seen in the 100 kHz trace) is evidence that this signal is indeed the flexural mode. A second feature worth noting is the prominent ringing of the transducer, as evidenced by the multi-burst nature of the first signal (as seen in the 100 kHz trace).

The LDV was used to measure the axial particle velocity for three distinct wires in the transmission line, specifically an outer aluminum wire, an inner aluminum wire, and an outer steel wire (locations a, b, and c in Fig. 5, respectively). Results for a 100 kHz excitation frequency are shown in Fig. 11. Clearly, elastic waves are also present in the inner wires, and hence, it is possible to detect breaks in these wires. The amplitude of the elastic waves becomes smaller at increasing distance from the surface due to the weak coupling of energy to the inner wires. The attenuation coefficient for the first longitudinal mode in the surface aluminum wire is estimated to be $k_2 = 0.27$ m^{-1}, meaning that the elastic wave will propagate approximately 12 m before the signal level falls below a measurable level (SNR < 2).

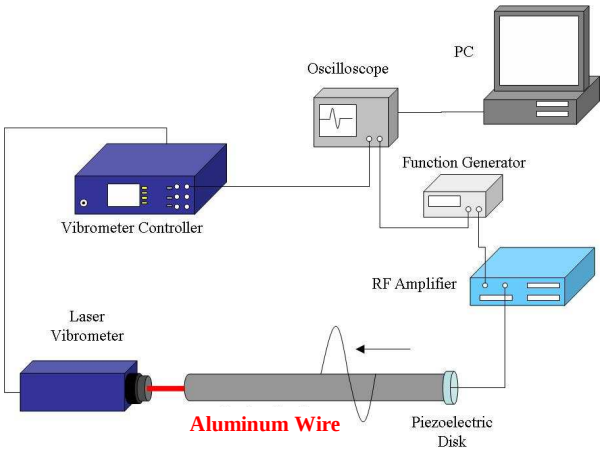

Fig. 6: Experimental setup for characterizing longitudinal waves in a single wire.

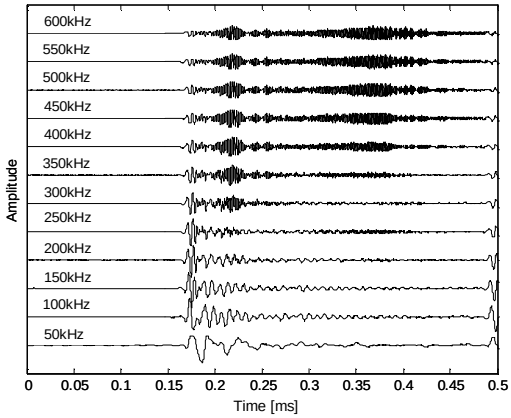

Fig. 7: LDV-measured axial particle velocity as a function of frequency.

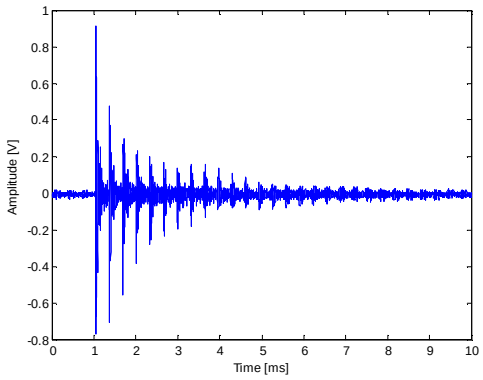

Fig. 8: Multiple reflections of a longitudinal wave in a single wire (100 kHz excitation).

5. DEFECT DETECTION

The main goal of this research is the monitoring of overhead transmission lines using elastic waves. In this section, two detection methodologies are considered. In section 5.1, a "global" scheme is described which uses a ring transducer to send elastic energy into every single wire in the transmission line. In section 5.2, a "local" scheme is described which utilizes smaller transducers for sending elastic energy into a select few surface wires.

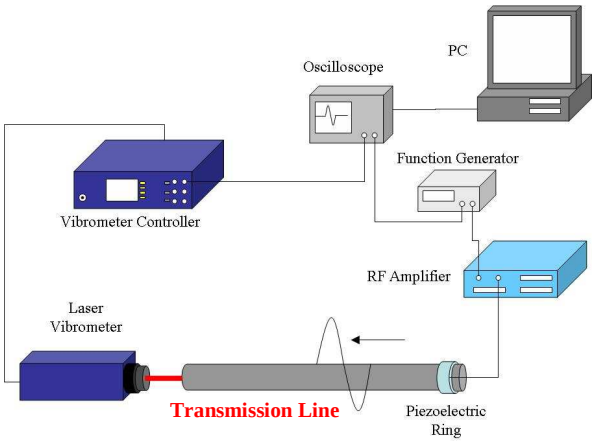

Fig. 9: Experimental setup for characterizing longitudinal waves in a transmission line.

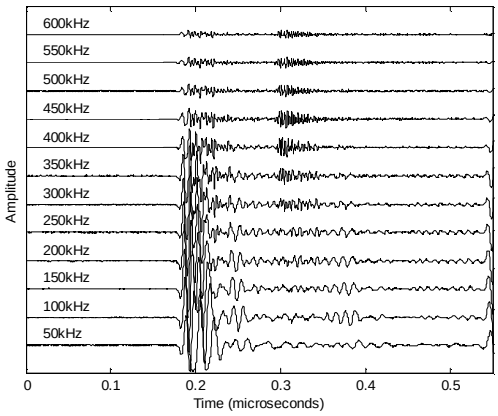

Fig. 10: LDV-measured axial particle velocity for a surface wire as a function of frequency.

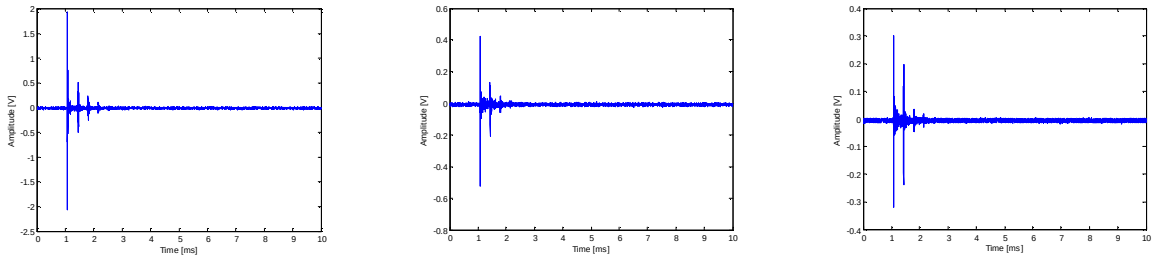

Fig. 11: LDV-measured axial particle velocity for an outer aluminum wire (left), an inner aluminum wire (middle), and an outer steel wire (right).

5.1. Global Detection

The experimental setup for global defect detection in a transmission line is shown in Fig. 12. As shown, a pulser-receiver drives the piezoelectric ring with an electrical spike input, which in turn generates an elastic wave in the transmission line. The piezoelectric ring, as it is attached to the transmission line, is illustrated in Fig. 13. The pulser-receiver then switches automatically from “send” to “receive” mode. The elastic wave is reflected from discontinuities in the transmission line, and the reflected wave is sensed by the piezoelectric ring. The signal from the ring is received and amplified by the pulser-receiver. Artificial damage in the form of a transverse cut is made using a handsaw. The cuts are made at a distance of 700 mm from the piezoelectric ring, and they range from 2 mm in depth to a complete cut.

The received signal for a 7 mm cut is compared to the undamaged case in Fig. 14. The two signals are nearly identical until ~ 0.3 ms. The reflection of the fundamental longitudinal wave from the cut is responsible for the difference in the two signals. The presence of a signal before the arrival of this reflection is caused by the ringing of the piezoelectric ring. That is, the ring continues to vibrate, thereby generating a voltage signal, even after the excitation has been removed. The maximum amplitude of the reflected wave as a function of cut depth is illustrated in Fig. 15. A linear relationship between the degree of damage and the maximum reflected wave amplitude has been observed. This relation could be used for monitoring purposes in order to identify the state of damage in a cable.

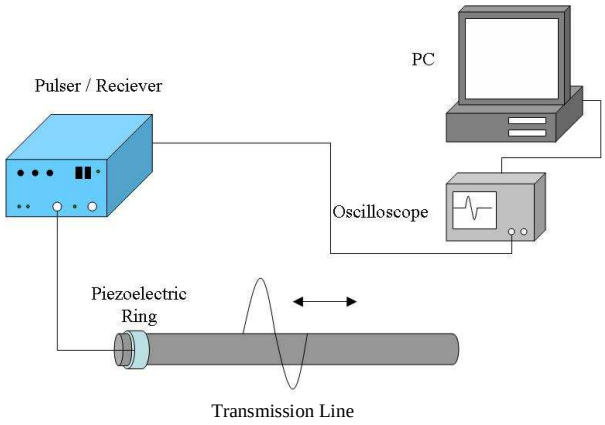

Fig. 12: Experimental setup for defect detection in the transmission line.

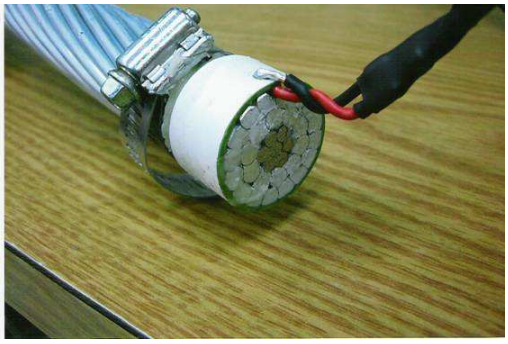

Fig. 13: Piezoelectric ring transducer attached to the transmission line.

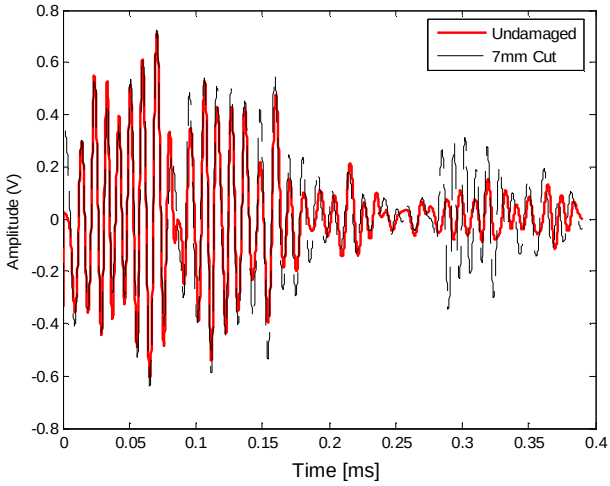

Fig. 14: Transducer output for a damaged and an undamaged transmission line.

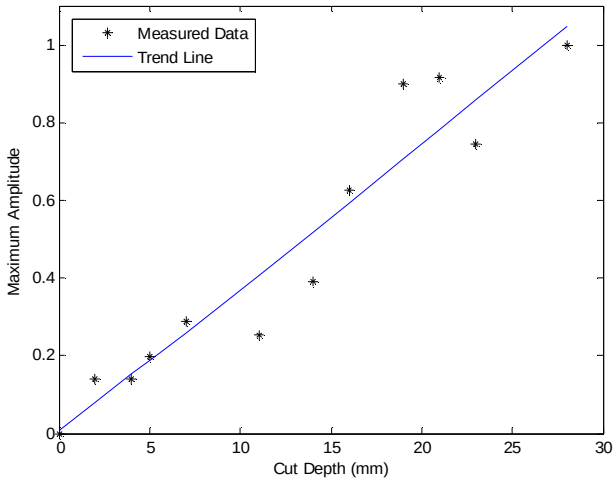

Fig. 15: Maximum amplitude of the reflected wave at various damage levels.

5.2. Local Detection

An alternative experimental setup for identifying wire breaks in an overhead power line is depicted in Fig. 16. As opposed to the transmission line considered in the previous sections, the transmission line here consists of a seven-wire stainless steel central load-bearing layer surrounded by 3 concentric layers of aluminum conductor wires (12, 18, 24 wires in the respective layers). The individual wires have diameters of 3.5 mm. Additionally, an artificial defect is generated by breaking a single surface wire at a distance of 780 mm from the sending transducer. Referring to Fig. 16, a function generator drives a sending transducer with a single cycle of a 500 kHz sinusoid. The sending and receiving transducers (10 mm diameter, piezoceramic material) are attached to the same surface wire on the transmission line (see Fig. 17). Experiments have shown that at this excitation frequency, the ultrasound is confined to the driven wire, so that no significant mode structure in the transmission line as a whole is produced. The sending transducer converts the input electrical energy into mechanical energy via the piezoelectric effect, and a transient stress wave is thereby generated in the surface wire. The stress wave propagates through the surface wire, is reflected at the surface break, and returns to the receiving transducer. The mechanical stress is converted into an electrical signal at the receiving transducer via the inverse piezoelectric effect. The signal is amplified, filtered, and finally sent to an oscilloscope for digital storage. The electrical output from the receiving transducer is depicted in Fig. 18. The initial signal burst (A) is referred to as the “main bang”. It corresponds to the stress wave which is

generated at the sending transducer and immediately sensed by the receiving transducer. Transducer ringing is evident in the main burst, but this ringing dies out relatively quickly. The second burst (B) corresponds to the stress wave which has been reflected from the surface break. Time of flight calculations are used to predict the location of the break, and this value accurately predicts the physical location of the break. The additional bursts (C-E) in the diagram correspond to longer propagation paths of the elastic wave. Attempts at locating subsurface wire breaks using a single transducer pair located on the surface remain unsuccessful. However, experimental findings hint at the feasibility of detecting subsurface breaks using surface excitation and detection.

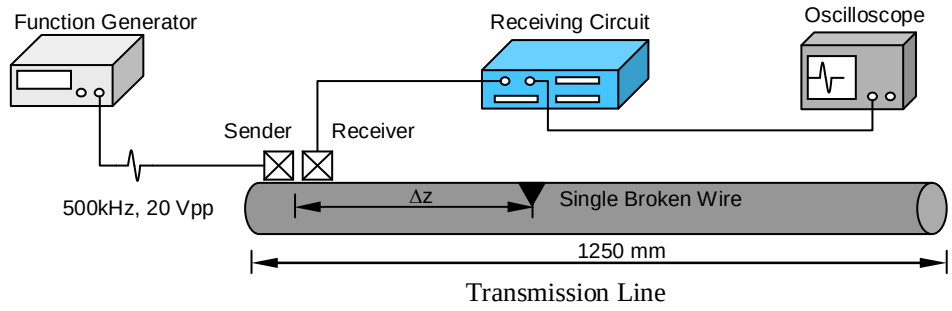

Fig. 16: Alternative experimental setup for defect detection in a transmission line.

Fig. 17: Disc transducers attached to a surface wire.

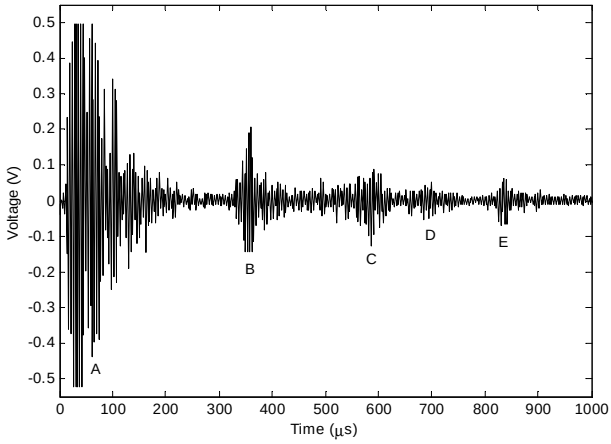

Fig. 18: Electrical output from the receiving transducer.

5.3. Comparison of Detection Methods

The global detection method (ring transducer) allows both inner and outer wires to be monitored, but ringing of the transducer is problematic. That is, continued vibration of the ring transducer, even after removal of the drive signal, causes generation of voltage which can mask defect-reflected signals. Future work includes development of passive mechanical or active electrical means of transducer damping.

The local detection method (small disc transducers) allows for clear identification of a single broken wire out of 61 using modest drive levels (20 V_{pp}) and a simple analog receiving circuit. Additionally, the 500 kHz excitation frequency (as opposed to 100 kHz) allows for better spatial resolution. The main disadvantage of the local method is that a complex array of transducers and an appropriate addressing scheme is required to interrogate all surface wires. Future work includes realization of such an array. Single array elements could be individually addressed in order to assess the health of the surface wires; and, subsurface wires could be interrogated by addressing multiple array elements

6. CONCLUSIONS

In this study, the feasibility of continuous, on-line monitoring of transmission lines using ultrasonic waves is considered. First the theory of guided waves in rods was introduced. Wave propagation in a single wire is complicated due to the multi-mode and dispersive nature of the guided waves and is even more complicated for a transmission line consisting of twisted wires of two different materials. Measurements in this study therefore focused on characterization of the fundamental longitudinal mode. Important results of this study include: a better understanding of the attenuation and dispersion phenomenon in transmission lines; and, the development of two methods for defect detection.

Additional feasibility studies are required in order to realize the ultimate goal of an autonomous monitoring system for overhead transmission lines. It is envisioned that a wireless communication system could be used to transmit data from the transducers to a base station. Additionally, energy harvesting methods (i.e., the use of solar energy or vibration energy to charge a battery), could be used to power the transducers and associated electronics (Hurlebaus and Gaul, 2006). An important feasibility study entails determining whether driving, receiving, and transmitting electronics would function in an environment having a high level of electromagnetic interference. Depending on interest and available funding, development of a prototype field unit for use on transmission lines could begin. Following the development of the prototype unit, field tests would have to be performed in order to test the device under real circumstances. The results of the current feasibility study can also be used to develop defect detection strategies for other cable structures.

7. REFERENCES

[1] Graff, K.F., Wave Motion in Elastic Solids, Dover Publications, Inc., New York, 1991.

[2] Hurlebaus, S. and Gaul, L., “Smart Structure Dynamics”, Mechanical Systems and Signal Processing, Vol. 20, No. 2, pp. 255-281, 2006.

[3] Meitzler, A.H., “Mode Coupling Occurring in the Propagation of Elastic Pulses in Wires”, Journal of the Acoustical Society of America, Vol. 33, No. 4, pp. 435-445, 1961.

[4] Rizzo, P. and Lanza di Scalea, F., “Monitoring Steel Strands via Ultrasonic Measurements”, Proceedings of SPIE - The International Society for Optical Engineering, Vol. 4696, pp. 62-73, 2002.

[5] Rizzo, P. and Lanza di Scalea, F., “Wave Propagation in Multi-wire Strands by Wavelet-based Laser Ultrasound”, Experimental Mechanics, Vol. 44, No. 4, pp. 407-415, 2004.

[6] Rizzo, P. and Lanza di Scalea, F., “Ultrasonic Inspection of Multi-Wire Steel Strands with the Aid of the Wavelet Transform”, Smart Materials and Structures, Vol. 14, pp. 685-695, 2005.

[7] Siegert, D. and Brevet, P., “Fatigue of Stay Cables Inside End Fittings: High Frequencies of Wind Induced Vibrations”, OIPEEC Bulletin 89, pp. 43-51, 2005.

[8] U.S. Helicopter summary statistics, Helicopter Association International, 1996-2004.

[9] Washer, G.A.; Green, R.E. and Pond, R.B., “Velocity Constants for Ultrasonic Stress Measurement in Pre-stressing Tendons”, Research in Nondestructive Evaluation, Vol. 14, pp. 81-94, 2002.

ACKNOWLEDGEMENT

The research group at Texas A&M University wishes to acknowledge support received from the National Institute for Occupational and Environmental Health (NIOSH)/Center for Disease Control and Prevention (CDC) under grant no. T42CCT610417. Funding was administered by the Southwest Center for Occupational and Environmental Health (SWCOEH), a NIOSH education and research center.

The research group at the University of Stuttgart wishes to acknowledge support received from PFISTERER Holding AG, Rosenstraße 44, 73650 Winterbach, Germany, www.pfisterer.com.